Conversion of ZnO Nanowires into Nanotubes with Tailored Dimensions

Jamil Elias, Ramon Tena-Zaera,* Guillaume-Yangshu Wang, and Claude Lévy-Clément

Institut de Chimie et Matériaux de Paris-Est, CNRS, UMR 7182, Bât. F, 2-8 rue Henri Dunant, 94320 THIAIS, France

Received April 25, 2008. Revised Manuscript Received August 7, 2008

An innovative route is presented to obtain arrays of single-crystal ZnO nanotubes with tailored dimensions. The three-step process combines electrochemical and chemical approaches. The first step consists in the electrodeposition of ZnO nanowire arrays from the O_2 reduction in an aqueous solution of zinc chloride ($ZnCl_2$) and potassium chloride (KCl). In the second step the core of ZnO nanowires is selectively etched in a KCl solution, resulting in the formation of tubular structures. The influence of KCl concentration, temperature, and immersion time in the ZnO nanotube formation process is investigated, with the finding that the dissolution of the nanowire core occurs for [KCl] ≥ 1 M and the etching rate is enhanced with the temperature. Arrays of ZnO nanotubes with tailored dimensions (200−500 nm external diameter and 1−5 μm length) are obtained by varying the conditions of nanowire array deposition and taking into account the dimensions of the nanowires to adjust the dissolution time. A precise control of the nanotube wall thickness is achieved by performing a further electrodeposition step. The whole process occurs at low temperature (80 °C) in aqueous chloride solution at neutral pH, in a couple of hours. The structural properties of obtained ZnO nanotubes are analyzed by transmission electron microscopy, showing their single-crystal character.

Introduction

In the emerging field of nanoscience and nanotechnology, arrays of one-dimensional (1D) ZnO nanostructures display a morphology which is key to improving the understanding of the physical properties of nanomaterials as well as to developing a new generation of nanostructured devices in different technologies such as optoelectronics,[1] solar cells,[2] gas sensing,[3] field emission,[4] piezoelectrics,[5] and microfluidics.[6] Although the research on ZnO nanowires is in advanced step with respect to that on nanotubes, the latter emerge as an interesting alternative due to the higher specific surface and porosity. Because the physical properties and device design may be determined by the nanotube dimensions, an important challenge is to obtain arrays of ZnO nanotubes with controllable dimensions. There are two main ways to obtain ZnO nanotubes, either by direct deposition or by conversion of nanowires into nanotubes. Few papers report on the direct deposition of ZnO nanotube arrays,[7] but the dependence on the local growth conditions (pressure, concentrations,...)[8] and state of substrates surface (cleaning, pretreatment,...)[9] is very strong resulting in ZnO nanotubes with poorly controlled dimensions. As ZnO nanowire arrays have been successfully deposited by several techniques,[10] and because their surfaces possess different chemical activities,[11] the selective dissolution of the nanowire core (from the top surface) in aqueous solutions is an interesting alternative to obtaining arrays of ZnO vertical nanotubes. Vayssieres et al.[12] demonstrated the feasibility of this approach in 2001. Nevertheless, the extremely long time (24

* Corresponding author. Tel.: +33(0)149781329. Fax: +33(0)49781203. E-mail: tena-zaera@icmpe.cnrs.fr.

(1) (a) Park, W. I.; Yi, G. C. *Adv. Mater.* **2004**, *16*, 87. (b) Konenkamp, R.; Word, R. C.; Godinez, M. *Nano Lett.* **2005**, *5*, 2005.
(2) (a) Lévy-Clément, C.; Tena-Zaera, R.; Ryan, M. A.; Katty, A.; Hodes, G. *Adv. Mater.* **2005**, *17*, 1512. (b) Law, M.; Greene, L. E.; Johnson, J. C.; Saykally, R.; Yang, P. *Nat. Mater.* **2005**, *4*, 455. (c) Martinson, A. B.; Elam, J. W; Hupp, J. T.; Pelin, M. J. *Nano Lett.* **2007**, *7*, 2183.
(3) (a) Tien, L. C.; Sadik, P. W.; Norton, D. P.; Voss, L. F.; Pearton, S. J.; Wang, H. T.; Kang, B. S.; Ren, F.; Jun, J.; Lin, J. *Appl. Phys. Lett.* **2005**, *87*, 222106. (b) Liao, L.; Lu, H. B.; Li, J. C.; He, H.; Wang, D. F.; Fu, D. J.; Liu, C.; Zhang, W. F. *J. Phys. Chem. C* **2007**, *111*, 1990. (c) Wei, A.; Sun, W.; Xu, C. X.; Dong, Z. L.; Yu, M. B.; Huang, W. *Appl. Phys. Lett.* **2006**, *88*, 213102.
(4) (a) Ye, C.; Bando, Y.; Fang, X.; Shen, G.; Goldberg, D. *J. Phys. Chem. C* **2007**, *111*, 12673. (b) Wang, X.; Zhou, J.; Lao, C.; Song, J.; Xu, N.; Wang, Z. L. *Adv. Mater.* **2007**, *19*, 1627.
(5) Wang, X.; Song, J.; Liu, J.; Wang, Z. L. *Science* **2007**, *316*, 102.
(6) Badre, C.; Pauporté, T.; Turmine, M.; Lincot, D. *Nanotechnology* **2007**, *18*, 365705.
(7) (a) Liang, H. W.; Lu, Y. M.; Shen, D. Z.; Li, B. H.; Zhang, Z. Z.; Shan, C. X.; Zhang, J. Y.; Fan, X. W.; Du, G. T. *Solid State Commun.* **2006**, *137*, 182. (b) Sun, Y.; Fuge, G. M.; Fox, N. A.; Riley, D. J.; Ashfold, M. N. R. *Adv. Mater.* **2005**, *17*, 2477. (c) Hu, J. Q.; Bando, Y. *Appl. Phys. Lett.* **2003**, *82*, 1401.
(8) (a) Zhang, B. P.; Binh, N. T.; Wakatsuki, K.; Segawa, Y.; Yamada, Y.; Usami, N.; Kawasaki, M.; Koinuma, H. *J. Phys. Chem. C* **2004**, *108*, 10899. (b) Yu, H.; Zhang, Z.; Han, M.; Hao, X.; Zhu, F. *J. Am. Chem. Soc.* **2005**, *127*, 2378.
(9) Tang, Y.; Luo, L.; Chen, Z.; Jiang, Y.; Li, B.; Jia, Z.; Xu, L. *Electrochem. Commun.* **2007**, *9*, 289.
(10) (a) Yi, C. C.; Wang, C.; Park, W. I. *Semicond. Sci. Technol.* **2005**, *20*, S22–S34. (b) Huang, M.; Wu, Y.; Feick, H.; Tran, N.; Weber, E.; Yang, P. *Adv. Mater.* **2001**, *13*, 113. (c) Ding, Y.; Gao, P. X.; Wang, Z. L. *J. Am. Chem. Soc.* **2004**, *126*, 2066. (d) Park, W. I.; Kim, D. H.; Jung, S. W.; Yi, G. C. *Appl. Phys. Lett.* **2002**, *80*, 4232. (e) Zuniga-Perez, J.; Rahm, A.; Czekalla, C.; Lenzner, J.; Lorenz, M.; Grundmann, M. *Nanotechnology* **2007**, *18*, 195303. (f) Vayssieres, L. *Adv. Mater.* **2003**, *15*, 464. (g) Könenkamp, R.; Boedecker, K.; Lux-Steiner, M. C.; Poschenrieder, M.; Zenia, F.; Levy-Clement, C.; Wagner, S. *Appl. Phys. Lett.* **2000**, *77*, 2575.
(11) Wang, Z. L.; Kong, X. Y.; Zuo, J. M. *Phys. Rev. Lett.* **2003**, *91*, 185502.
(12) Vayssieres, L.; Keis, K.; Hagfeldt, A.; Lindquist, S. E. *Chem. Mater.* **2001**, *13*, 4395.

10.1021/cm801131t CCC: $40.75
Published on Web 10/10/2008

h)[12] necessary to convert nanowires into nanotubes limited the applicability of this method to laboratory scale processes. Some routes[13−17] have recently been proposed to enhance the dissolution rate of the nanowire core and decrease therefore the time period necessary for the nanotube formation. She et al.[15] reported very interesting results, obtaining nanotubes from electrodeposited ZnO nanowire arrays in ∼2 h by using hydrochloric (pH ∼ 3) and potassium hydroxide (pH ∼ 13) aqueous solutions. The pH values of the etching solutions may induce some corrosion problems and limit therefore the substrate choice. But more important, no control on the nanotube wall thickness was reported.

Here, we present a new strategy for fabricating arrays of vertically aligned single-crystal ZnO nanotubes on transparent conducting oxide substrates with tailored dimensions (external diameter, wall thickness, and length), by combining electrochemical and chemical approaches. The whole process occurs at relatively low temperature (80 °C) in aqueous chloride solution at neutral pH avoiding possible problems related to the chemical stability of the substrates.

Experimental Section

Electrodeposition of ZnO Nanowire Arrays. The electrodeposition of ZnO nanowire arrays was performed in a three-electrode electrochemical cell. The cell was made up of the substrate, which is a conducting glass covered by a sprayed buffer layer of ZnO to make a glass/SnO_2:F/ZnO_{sp} surface, as the cathode or working electrode, a Pt spiral wire as the counter electrode, and a saturated calomel electrode (SCE) as the reference electrode. Experimental details on the deposition of the sprayed ZnO layer can be found elsewhere.[18] For each working electrode, an area of 2 cm^2 was masked off prior ZnO nanowire arrays were deposited on top of the sprayed ZnO buffer layer.

The electrolyte was an aqueous solution of 5×10^{-4} M $ZnCl_2$ and 3.4 M KCl at pH 7. The solution was saturated with bubbling oxygen 10 min before and during the deposition. The ZnO nanowire arrays were electrodeposited at a potential of −1 V versus SCE in 80 °C electrolyte solution, using an Autolab PGSTAT-30 potentiostat. Charge density was 2.5 or 10 C/cm^2. Ultrapure water (18 MΩ·cm) was provided by a Millipore setup. Anhydrous $ZnCl_2$ salt (Flucka, purity >98.0%) was used as the Zn^{2+} precursor. KCl (Flucka, purity >99.5%) served as a supporting electrolyte, among other roles.[19]

Dissolution of the Core of ZnO Nanowires. After the electrodeposition of ZnO nanowire arrays, the samples were immersed in KCl solution of concentration in the range from 0.1 to 3.4 M for time periods ranging from 0.5 to 9 h. The temperature of the solution was varied from 25 to 80 °C. The immersion time was optimized taking into account the nanowire dimensions in 3.4 M KCl solution at 80 °C.

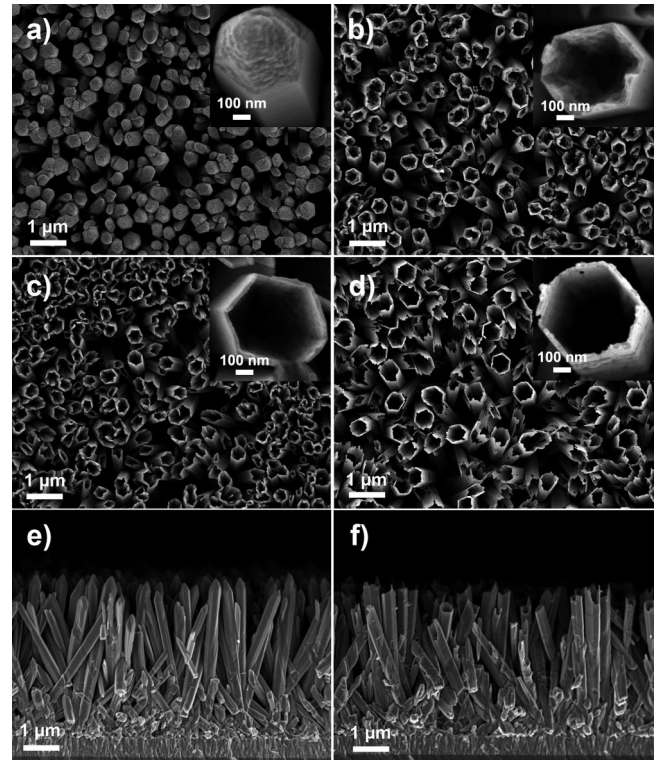

Figure 1. SEM micrographs of (a) an as-deposited ZnO nanowire array; (b−d) those immersed in different [KCl] aqueous solutions (1, 2, and 3.4 M, respectively) during 3 h at 80 °C. Insets show high-magnification images of a single 1D ZnO nanostructure. Panels e and f correspond to cross sections of arrays shown in panels a and d, respectively.

ZnO Electrodeposition on ZnO Nanotube Arrays. The second electrodeposition was performed in the same experimental conditions as those of the first step (except [KCl] = 0.1 M instead 3.4 M), using the ZnO nanotube array as a cathode.

Physical Characterization. The morphology of ZnO nanowires and nanotubes was analyzed using a field emission scanning electron microscope (SEM) LEO 1530. Some ZnO nanotubes were scratched off the substrate to analyze their structural properties by transmission electron microscopy (TEM) using a high-resolution Topcon EM 002B microscope operating at 200 kV. A drop of an ethanol suspension containing the nanowires was deposited on a copper grid with lacey carbon for TEM observations.

Results and Discussion

Figure 1a shows an SEM image of a nanowire array obtained after passing a charge density of 10 C/cm^2. From a statistical analysis of top-view and cross-sectional SEM micrographs,[20] the mean values of the diameter and the length of the nanowires were estimated to be ∼500 nm and ∼4 μm, respectively.

Previous work suggested that the adsorption of chloride ions (Cl^-) plays a major role during the electrodeposition of ZnO nanowire arrays.[19] Although Cl^- adsorption onto ZnO may be enhanced by applying an external potential,[20] it might also occur and play therefore a role after the end of the electrodeposition. To gain further insight into this matter, ZnO nanowire arrays were immersed in KCl solution and the effect of solution composition on the morphology was

(13) Yan, C.; Xue, D. *Electrochem. Commun.* **2007**, *9*, 1247.
(14) Yu, Q.; Fu, W.; Yu, C.; Yang, H.; Wei, R.; Li, M.; Liu, S.; Sui, Y.; Liu, Z.; Yuan, M.; Zou, G.; Wang, G.; Shao, C.; Liu, Y. *J. Phys. Chem. C* **2007**, *111*, 17521.
(15) She, G.; Zhang, X.; Shi, W.; Fan, X.; Chang, J. C.; Lee, C.; Lee, S.; Liu, C. *Appl. Phys. Lett.* **2008**, *92*, 053111.
(16) Xu, L.; Liao, Q.; Zhang, J.; Ai, X.; Xu, D. *J. Phys. Chem. C* **2007**, *111*, 4549.
(17) She, G.; Zhang, X.; Shi, W.; Fan, X.; Chang, J. C. *Electrochem. Commun.* **2007**, *9*, 2784.
(18) Elias, J.; Tena-Zaera, R.; Lévy-Clément, C. *Thin Solid Films* **2007**, *515*, 8553.
(19) Tena-Zaera, R.; Elias, J.; Wang, G.; Lévy-Clément, C. *J. Phys. Chem. C* **2007**, *111*, 16706.
(20) Elias, J.; Tena-Zaera, R.; Lévy-Clément, C. *J. Phys. Chem. C* **2008**, *112*, 5736.

systematically studied. Samples were held for 3 h at 80 °C in solutions with 0.1, 1, 2, and 3.4 M KCl. No significant changes in the external diameter (Figure 1a−d) and length (Figure 1, parts e and f) between the resulting nanostructures and starting nanowires were observed. However, a partial dissolution of the nanowire core occurred for [KCl] ≥ 1 M (Figure 1b−d), resulting in partially or entirely hollow structures. A variation of the depth of the hole with the KCl concentration can be inferred from Figure 1, suggesting that chloride ions play a major role on the dissolution of the ZnO nanowire core. ZnO possesses two oppositely charged polar surfaces perpendicular to the [0001] direction. These surfaces are terminated exclusively by Zn^{2+} or by O^{2-} on the (0001) and (000$\bar{1}$) ZnO surfaces, respectively, and induce a net electrostatic dipole moment parallel to the *c*-axis. The stability of the (0001) and (000$\bar{1}$) ZnO surfaces requires that they become less positive and negative, respectively.[21] The typical ZnO crystal habit exhibits a basal (000$\bar{1}$) surface, a top (0001) surface, and nonpolar (10$\bar{1}$0) surfaces parallel to *c*-axis.[22] If this scenario is assumed for electrodeposited ZnO nanowires, Cl^- ions might be preferentially adsorbed onto the top of the nanowires to decrease the positive charge density of the (0001) ZnO surface. Because the (10$\bar{1}$0) faces appear to be the most stable ZnO surface,[23] chloride adsorption onto lateral walls seems to be less probable. The adsorption of Cl^- onto (0001) ZnO surface (zinc-terminated) may result in the formation of a highly water-soluble zinc chloride complex such as $ZnCl^+$, inducing the gradual dissolution of the nanowire core from the tip toward the bottom. Thus, varying the chloride concentration appears to be an efficient strategy to establish a method to convert ZnO nanowires into nanotubes. It is worth noting that no nanotube formation was observed in annealed (1 h at 450 °C in air) ZnO nanowire arrays. She et al.[15] observed a similar behavior and invoked a uniform distribution of defects after annealing versus a higher local defect density in the core of as-deposited nanowires to explain the absence of the nanotube formation for the annealed nanowires. Although the defects may play an important role in the nanotube formation, this hypothesis seems to be unlike probable because ZnO nanowires exhibit generally the highest defect density on their surface.[24] The annealing treatment could induce other phenomena, such as the surface reconstruction, that enhance the stability of (0001) ZnO surface[25] and impede therefore the nanotube formation.

In order to investigate the dissolution process, the time and temperature dependence of dissolution was also studied. A study of the dissolution time was performed with a solution of 3.4 M KCl at 80 °C. Figure 2 shows the morphology for two different times (0.5 and 5 h). As can be seen in Figure 2a, a dissolution time of 0.5 h resulted in the partial dissolution of the core just at the tip. The depth of the hole increases with time as shown by comparing samples immersed for 0.5 and 3 h (Figures 2a and 1d, respectively). No significant variations of the hole width were observed. For immersion times greater than 3 h, the degradation of lateral walls occurred (Figure 2b, time = 5 h). For times longer than 9 h, the ZnO nanostructures were fully dissolved and only the TCO substrate remained. The influence of temperature was also analyzed in the range from 25 to 80 °C, showing that dissolution rate increases with the temperature. This is not surprising as the increase of the temperature may enhance the chloride adsorption and solubility of zinc chloride complexes in water.

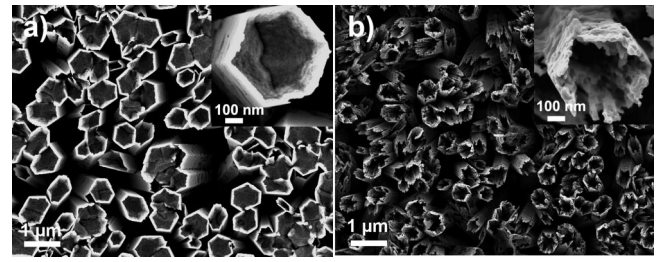

Figure 2. SEM micrographs of samples immersed in 3.4 M [KCl] aqueous solutions during different times: (a) 0.5 and (b) 5 h at 80 °C.

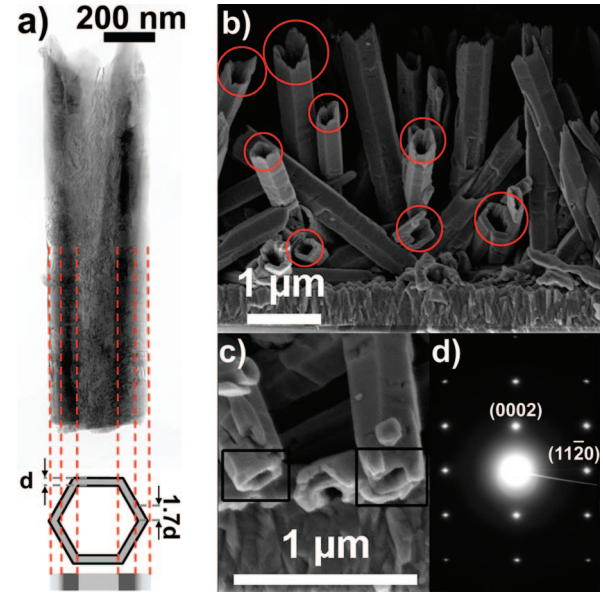

Figure 3. (a) Bright field TEM image of a single ZnO nanotube removed from the array shown in Figure 1d. A schematic view of a cross section of a hexagonal nanotube (d_{wall} ∼ 30 nm) is coupled to the TEM image to facilitate its understanding. (b) SEM micrographs of the cross section of an array that exhibits some nanotubes cut at different heights. Circled areas show that the nanotubes are hollow. (c) Magnification view of the base of some nanotubes detached from the substrate. Rectangular areas highlight the hollow base of the nanotubes. (d) SAED pattern from the nanotube of panel a.

The structural properties of ZnO nanotubes were analyzed by TEM. Figure 3a shows a bright field TEM image of one nanotube removed from the array of Figure 1d. The transversal variation of contrast can be explained by considering the differences in the effective thickness for the electrons crossing a hexagonal nanotube with a wall thickness (d_{wall}) of ∼30 nm. The darkest part corresponds to the largest effective thickness (∼3.4d_{wall} versus to 2d_{wall} in the middle of the nanotube). However, the differences in contrast along the longitudinal direction are due to the accidental partial

(21) Noguera, C. *J. Phys.: Condens. Matter* **2000**, *12*, R367.
(22) Li, W. J.; Shi, E. W.; Zhong, W. Z.; Yin, Z. W. *J. Cryst. Growth* **1999**, *203*, 186.
(23) Meyer, B.; Marx, D. *Phys. Rev. B* **2003**, *67*, 035403.
(24) Djurisic, A. B.; Leung, Y. H. *Small* **2006**, *2*, 944.
(25) (a) Liao, X.; Zhang, X. *J. Phys. Chem. C* **2007**, *111*, 9081. (b) Wander, A.; Harrison, N. M. *J. Chem. Phys.* **2001**, *115*, 2312.

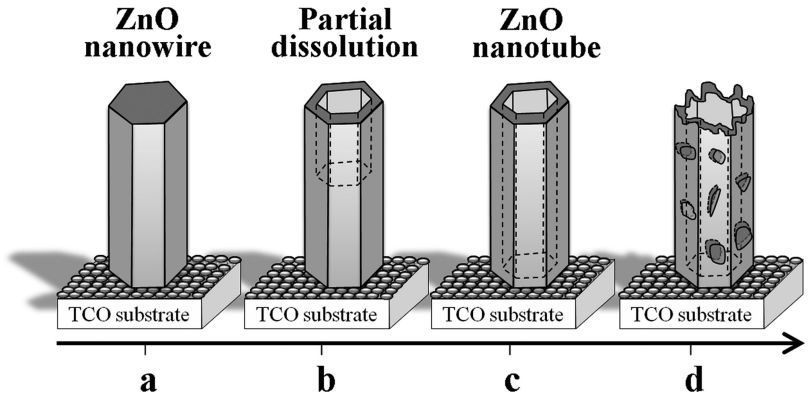

Figure 4. Schematic view of the dissolution process. Parts a and d correspond to the shortest and longest dissolution periods, respectively.

detachment of the wall and the resulting decrease in the effective thickness for electrons in the upper part of the nanotube. As discussed in the Experimental Section, TEM characterization was performed on nanotubes scratched off the substrate. This process induced multiple fractures, especially perpendicular to the longitudinal axis, making it difficult to show a convincing TEM image about the complete transformation from nanowires into nanotubes. As an example, the nanotube shown in Figure 3a is much shorter (~1.5 μm) than the mean length of the 1D nanostructures of the array (Figure 1f, ~4 μm). However, a complete conversion can be inferred from the given SEM micrographs of the cross sections (Figure 3, parts b and c). Figure 3b shows an SEM micrograph of a cross section of an array constituted of nanotubes accidentally cut, during the cross section preparation, at different heights (circled areas). Even the nanotubes that are cut at only few hundreds of nanometers above the substrate are hollow suggesting the complete conversion into tubes. This is confirmed in Figure 3c that shows two detached nanotubes with a hollow base (rectangular areas). Concerning the crystallinity of the nanotubes, selected area electron diffraction (SAED) experiments were performed. Figure 3d displays an electron diffraction pattern from the nanotube of Figure 3a. The diffraction pattern shows the hexagonal wurtzite structure, with the [0001] axis parallel to the longitudinal axis, and the single-crystal character of the ZnO nanotube. Therefore, the selective dissolution of the nanowire core does not seem to affect the crystallinity of either the rest of the nanowires or the obtained nanotubes.

According to the experimental observations, the evolution of the dissolution process is schematically summarized in Figure 4. The dissolution starts from the tip of the nanowires toward their bottom. The dissolution affects the nanowire core preferentially, leaving the lateral faces, resulting in a tubular structure. Degradation of the lateral walls starts when the core is fully dissolved, inducing a decrease of the length of the nanotubes until the complete dissolution of the ZnO nanostructures. The scheme of Figure 4 is valid for a wide range of KCl concentrations (1−3.4 M) and temperatures (25−80 °C). In the present route (pH ~ 7) the hole width stays constant without respect to time, except after long periods when degradation of the lateral walls begins. The "dissolution habit" seems to be similar to that reported by She et al.[15] in acidic (0.001 M HCl) and alkaline (0.125 M KOH) media. However, this differs from that of other

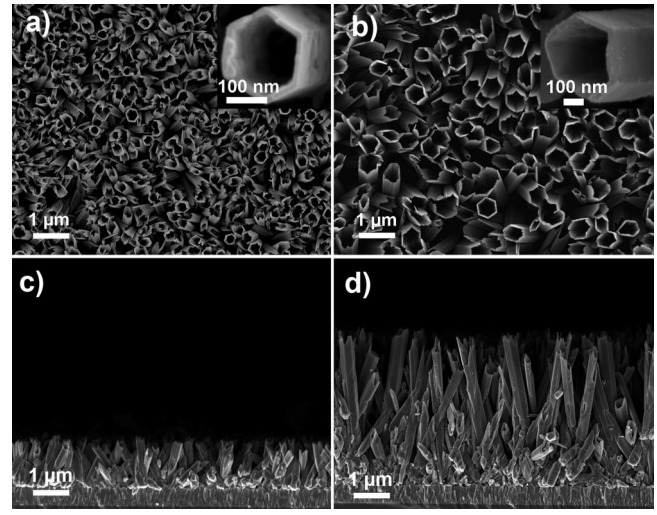

Figure 5. SEM micrographs of two nanotube arrays with different dimensions obtained from nanowire arrays electrodeposited by passing a charge density during the first step of the process: (a and c) 2.5 C/cm^2 and (b and d) 10 C/cm^2.

previously studied strategies. Yan and Xue[13] showed that dissolution in an acidic medium (pH ~ 2.6) starts at the corners of the hexagonal top surface of ZnO nanowires, generating six holes that widen gradually to dissolve the core fully. Xu et al.[16] also observed an augmentation of hole width with time by using an alkaline etchant (pH ~ 11.6).

As the dimensions of the electrodeposited ZnO nanowires can be tailored by varying the electrodeposition parameters,[19−21,26] the present route offers wide control over both the external diameter and the length of the nanotubes. SEM micrographs of two arrays of nanotubes with different external diameters, ~200 and 500 nm, and lengths, 1.3 and 4 μm, respectively, are shown in Figure 5. Different dimensions were successfully obtained by modifying the charge density passed during electrodeposition (2.5 or 10 C/cm^2) and taking into account the dimensions of the nanowires to adjust the dissolution time. With respect to nanotube walls, it is worth noting that the hole width is slightly affected by the KCl concentration (Figure 1). Wall thicknesses from 20 to 45 nm were obtained in a controlled manner by taking advantage of the influence of [KCl]

(26) Elias, J.; Tena-Zaera, R.; Lévy-Clément, C. *J. Electroanal. Chem.* **2008**, *621*, 171.

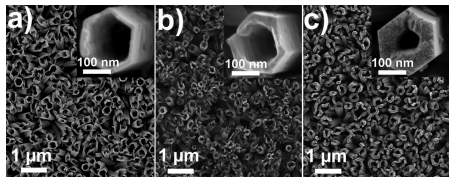

Figure 6. SEM micrographs of ZnO nanotube arrays: (a) after dissolution of the core of ZnO nanowires (second step); (b and c) ZnO nanotube arrays after further ZnO electrochemical deposition (third step; b, 2.5 C/cm^2 and c, 10 C/cm^2).

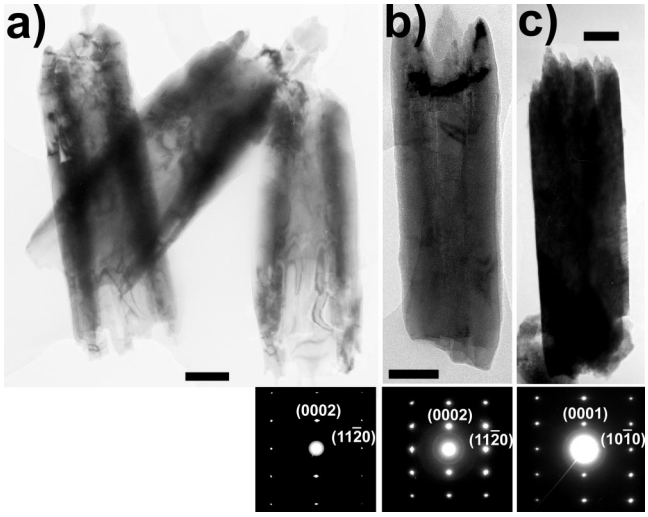

Figure 7. Bright field TEM images of ZnO nanotubes removed from the arrays shown in (a) Figure 6a, (b) Figure 6b, and (c) Figure 6c. The scale bars are 100 nm in length. The electron diffraction patterns are also shown of each single nanotube. The SAED experiments were performed in the (a and b) [21$\bar{3}$0] and (c) [11$\bar{2}$0] zone axes.

(Figure 1 of the Supporting Information). Nevertheless, the variation range seems to be limited to several nanometers (∼25 nm).

Then, in order to enhance the control of the thickness of the nanotube wall, a third step that consisted in a second ZnO electrodeposition in a $ZnCl_2$ solution was included in the process. The third step allowed a precise monitoring of the thickness of the nanotube wall in a wide range. As an example, Figure 6 shows the SEM micrographs of the arrays of nanotubes, with different wall thicknesses (20−85 nm), obtained by modifying the charge density passed during the last electrodeposition step. Although nanotubes exhibit size dispersion, no significant changes in the mean values of external diameter (∼220 nm, Figure 6a−c) and in length (∼1.1 μm, Figure 2 of the Supporting Information) were observed, suggesting that the ZnO was only deposited on the (10$\bar{1}$0) inner nanotube walls. This was supported by an additional experiment performed to fill completely the nanotubes. This was attained by increasing the charge density passed during the third step, and differences smaller than 10 nm were observed between the mean value of the external diameter of the as-formed nanotubes and that of the resulting nanowires (Figure 3 of the Supporting Information).

The structural properties of ZnO nanotubes obtained after the third step were also analyzed by TEM. Figure 7 summarizes the results from the TEM characterization of nanotubes of the arrays shown in Figure 6. Bright field TEM images show a clear contrast variation for the as-formed nanotubes (Figure 7a), whereas the contrast differences are weak and nonobservable for nanotubes obtained after a relatively short (2.5 C/cm^2, Figure 7b) and long (10 C/cm^2, Figure 7c) third step, respectively. This can due to the increase of the wall thickness; nanotubes with $d_{wall} \sim 85$ nm seem to be too thick for electrons even along the smallest effective thickness ($2d_{wall}$). Electron diffraction patterns show the single-crystal character of the nanotubes, demonstrating that they are also single crystals even after the third step. This is also supported by X-ray diffraction (XRD) experiments, where the analyzed sample area is larger, because significant variations in the preferential orientation (expected for a multicrystalline coating) were not observed between the XRD patterns of nanotube arrays obtained after the second and third step (Supporting Information, Figure 4). The single-crystallinity is an important advantage of the present method with respect to template-based routes, previously used to tailor the nanotube dimensions, which generally result in polycrystalline ZnO nanotubes.[27]

Thus, the present combined route allows the fabrication of arrays of single-crystal ZnO nanotubes with tailored dimensions in a couple of hours. Though the present three-step experiment has been performed in different solutions, the whole process could be optimized to take place in the same solution without any handling of the samples between the different steps, facilitating the adaptation to large-scale production. This is an important advantage with respect to other routes reported in the literature, which use different solutions for the nanowire deposition and nanotube formation.[15]

Conclusions

In summary, a low-temperature route (80 °C) to obtain arrays of single-crystal ZnO nanotubes with tailored dimensions has been presented. The method combines electrochemical and chemical approaches in neutral pH aqueous chloride solution. Arrays of ZnO nanotubes with a wide range of external diameters (200−700 nm) and lengths (1−5 μm) have been obtained after two-step process. A precise control of the nanotube wall thickness has also been achieved by performing a further electrodeposition step. Similar strategies can be added as a complementary step to the routes previously proposed on the literature to convert ZnO nanowires into nanotubes.[13,15−17] The present paper not only reports on an innovative route to dissolve selectively the core of ZnO nanowires but also offers possibilities to modify the wall thickness of the nanotubes obtained by previously reported methods.

Supporting Information Available: XRD patterns and some additional SEM micrographs of the ZnO nanotube arrays. This material is available free of charge via the Internet at http://pubs.acs.org.

CM801131T

(27) (a) Li, L.; Pan, S.; Dou, X.; Zhu, Y.; Huang, X.; Yang, Y.; Li, G.; Zhang, L. *J. Phys. Chem. C* **2007**, *111*, 7288. (b) Seo, B. I.; Shaislamov, U. A.; Ha, M. H.; Kim, S.-W.; Kim, H.-K.; Yang, B. *Physica E* **2007**, *37*, 241.